



Measuring Contour Similarity Based on Improved Hausdoff Distance for the Automatic Conjugation of Irregular Fragments of Ancient Manuscripts

Zixuan Yin and Yutong Zheng (✉)

School of Information Engineering, Minzu University of China, Beijing 100081, China
9900572@muc.edu.cn

Abstract. Ancient manuscripts have precious value in historical, cultural, social, and artistic. It is the common wealth of humanity. Suffering the long-term erosion and wears, ancient manuscripts were damaged and even completely separated into fragments scattered throughout the world. Fragment conjugation is an important part of the research and protection of ancient literature, However, the most advanced technology has not been adopted. Because we don't yet know how to make the entire work automated, and the design and use of similarity assessment indicators, which play a crucial role in automation. In this paper, we propose a contour similarity evaluation based on improved Hausdoff distance, and a novel model which can make entire conjugation fully automated. We took Dunhuang ancient manuscripts as an example, verified on fragmented datasets and compared with expert results. The results indicate that our method can work automated, and the success rate of conjugation has been significantly improved compared to existing methods for similar tasks; In the analysis of contour similarity evaluation, our method based on improved Hausdoff distance can effectively avoid missed matching and improve the success rate of matching.

Keywords: Ancient manuscript fragments · Dunhuang manuscripts · Contour similarity · Automatic conjugation model

1 Introduction

China has a long history which left a abundance of ancient manuscripts, while a majority of them are fractured and can be barely recognized. Ancient manuscripts are not only important to literature, but also to religion, linguistics, phonology, and sociology. The recovered manuscript will provide valuable information for related research of history and ancient culture. However, traditional conjugation work mainly relies on manual work and human power. Researchers must possess extensive professional knowledge and rigorous academic training, while the job itself requires a high degree of sensitivity and excellent memory.

With the development of image processing technology, the fully automatic conjugation of ancient manuscript fragments has become possible. We proposed a fully automatic conjugation method for ancient manuscript fragments, and takes the Dunhuang ancient manuscript fragments as an example for discussion.

2 Relative Work

There are many forms of fragment conjugation. Of all the literature around the world, there is little research on the conjugation of Dunhuang manuscript fragments. However, among other fields, there are relative studies, such as broken documents in criminal investigation and cultural relics for archaeological use.

Many scholars studied fragment conjugation and have certain achievements mainly in feature utilization and matching strategies. For feature utilization, some are based on the geometric feature of fragments, such as sharp point, sharp angle, area feature, corner feature and angle sequence feature of fragment edge. Since most ancient manuscript fragments are damaged, their edges are not clear. Therefore, if only the boundary characteristics are used for conjugation, the result may not be ideal. The other part is based on the content characteristics of fragments. Luo Zhizhong [11] proposed a fragment semi-automatic conjugation algorithm based on the character line and table characteristics. It is based on the boundary intersection distance, which needs artificial interference during the process. This algorithm has its rationality, but also limitations: it is not suitable for the conjugation of complex fragments, while the automation level is low. Liu Qiuju et al. [5] proposed that taking the number of continuous points of the boundary text as the text feature, and then using the continuous eight connectivity to extract the gray feature of the boundary text and construct the model for conjugation. Liu Xianguo et al. [6] proposed a conjugation method based on gray value matrix for document fragments, which performs dynamic clustering and inter class sorting according to text line characteristics. These are based on the characteristics of the fragment text itself, not the geometric characteristics of the fragment boundary.

Compared to local feature utilization, there is even less research on global matching strategy. Kimia B of Brown University [4] proposed an automatic fragment conjugation algorithm based on elastic matching. Although accuracy is relatively high, the algorithm's time efficiency is not as effective because of the complex process of multi-stage dynamic programming. Leitao [1] expresses the fragment images by the curvature of sampling points of the fragment's contour. It uses multi-scale strategy to find the best match. Due to the complexity of the process, the time efficiency of the algorithm is relatively low. Leitao [1] also studies the multi-scale method to solve the fragment matching problem of two-dimensional plane image. Kang Zhang et al. [12] proposes a matching algorithm based on feature points, which performs global matching based on local matching translation rotation relationship.

Other scholars have also studied semi-automatic conjugation. Patrick [19] uses the chain code algorithm to track the contour of each fragment for matching, which adopts a semi-automatic conjugation method of human-computer interaction. Lu Yuhong [10] discusses a series of algorithms for the conjugation of broken paper, which proposes minimal manual intervention as a useful attempt to promote it to general problems.

In other research fields, Tsamoura E [9] proposes an improved fragment conjugation algorithm based on color matching, which takes oil painting as the research object. Papaodysseus [8] aims at the problem of repairing mural fragments, which extracts the most possible information from the contour shape of the fragment in any initial complete plane object to point out the possible fragment matching.

3 Automatic Conjugation Model

3.1 Automatic Conjugation Model

The overall structure of the automatic conjugation model is shown in Fig. 1, which includes parts such as fragment image normalization, contour similarity evaluation, and conjugation evaluation based on multi-layer feature fusion. The purpose of fragment image normalization is to assist in completing the extraction of fragment features and establishing the conjugation plane. Local matching based on contour features includes contour feature extraction, feature matching, and evaluation, which is used to complete rough matching. The multi-layer feature evaluation stage integrates physical layer and semantic layer information. Finally, the contour matching results are further confirmed and evaluated through multi-layer feature matching, and the fragment conjugation is performed according to the matching results.

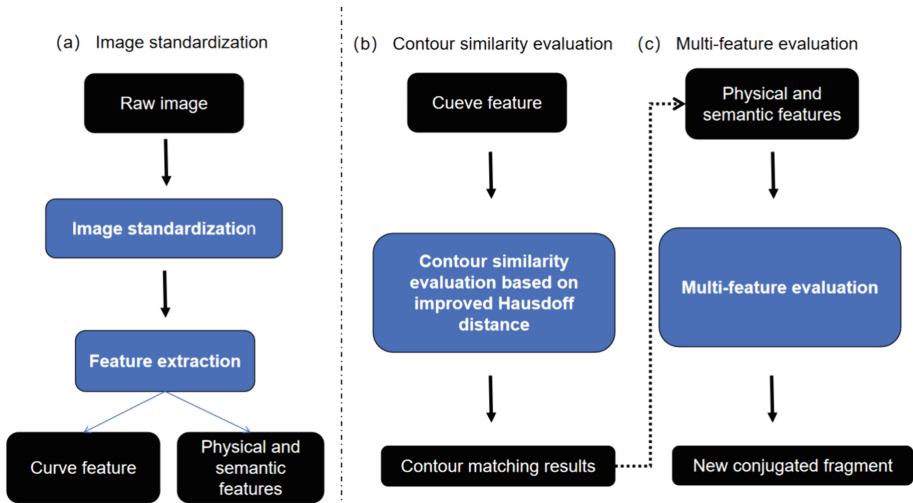


Fig. 1. Automatic conjugation model

Fragment Image Standardization. The aim of image standardization is to extract the effective information that can be used for matching from different fragment images. It mainly includes fragments normalization, establishment of conjugation vector and so on. For the i -th fragment image:

- 1) Establishing a local coordinate system for fragment i : By means of denoising, morphological processing, and edge extraction, the closed contour curve with single pixel for fragment i is obtained. The curve is then subjected to polygonal fitting to obtain the polygon w_i and its edge point set.

$$V_i = \{v_1(x_1, y_1), v_2(x_2, y_2), \dots, v_n(x_n, y_n)\}$$

Calculate the centroid of w_i and set it as the origin of the local coordinate system of fragment i . Then, based on the Hough transform, identify the direction of the text and set it as the positive y -axis direction (up and down). The positive x -axis is clockwise perpendicular to the y -axis. Establish a local coordinate system for the purpose of facilitating the subsequent acquisition of the relative position of the fragment and unifying the orientation of the fragment image for automatic alignment.

- 2) The fragments stored in collection institutions around the world have different specifications. As shown in Figure 2, the matching effect will be affected by the fragment images of different sizes and resolutions, thus requiring image scaling.

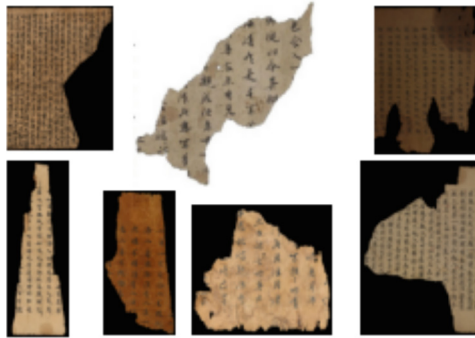


Fig. 2. Ancient Manuscript fragments

We extract characters from the image and determine the standard character size. Then, we compare all fragmented characters with the standard character and calculate the scaling factor, $scale_i$. We adjust all images according to $scale_i$ to ensure that the text size on the merged fragments is the same, with the aim of eliminating the impact of inconsistent image proportions caused by factors such as shooting angle, shooting height, and shooting equipment. The entire process is divided into two steps: fragment character segmentation and image size adjustment.

Firstly, regarding character segmentation, we adopt the projection method, which uses the number of pixels in the projection as the basis for character segmentation. This includes:

- a) Binary image processing.

$$dst(x, y) = \begin{cases} 0, & src(x, y) \geq thresh \\ 255, & src(x, y) < thresh \end{cases} \quad (1)$$

In the equation, “dst” represents the threshold segmentation result image, which has the same size and type as the original image. “src(x,y)” denotes the pixel value of the source image at the coordinate (x,y). “thresh” is the threshold value used for image segmentation.

- b) Before projection, morphological adjustment should be performed by conducting A dilation operation on set B in set z^2 . The dilation of set B with respect to set A is defined as follows.

$$A \oplus B = \{z | (\hat{B})_z \cap A \neq \emptyset\} \tag{2}$$

In the formula, “A” represents the inflated set (image object), while “B” denotes a structuring element. \hat{B} is the reflection of “B”. The equation indicates that the intersection of the translation of the reflection of “B” and “A” is not empty.

- c) Horizontal projection and vertical projection.
- d) Character segmentation.

The result of the segmentation is shown in Fig. 3:



Fig. 3. Character segmentation result

Ideally, the box should be a word for a box, but by observing Fig. 3, there are excessive segmentation and adhesion of the character segmentation. Considering the complexity of Chinese structure and the relative irregularity of handwritten characters, the Ratio of width to height of split box is limited. The aspect Ratio limit is set to $0.9 \leq \text{Ratio} \leq 1.1$. After the improvement of character segmentation as shown in the Fig. 4, over-segmentation, adhesion phenomenon is significantly reduced.

The character segmentation results in the following sequence of segmentation boxes:

$$Res = \{(h_1, w_1), (h_2, w_2), \dots, (h_n, w_n)\}$$

H_K, W_K is the height and width of the split box, and the maximum value is selected as the reference data H and W.

Based on the standard character size, we calculate the scale $Scale_i$ and adjust the size of the fragment image. The scale of the Shard image is:

$$Scale_i = \frac{H}{(h + w)/2} \tag{3}$$



Fig. 4. The filtered character segmentation result

In the formula, H is the number of pixels on the side of the selected standard character. If the $Scale_i$ is greater than 1, the image needs to be up-sampling adjustment; less than 1, the image needs to be down-sampling adjustment.

Build the conjugation vector A_i of fragments i : for each fragments i , we extract the outer contour W_i and the point set V_i , and calculate the fragments area A_i . The conjugation vector A_i includes centroid, set of exterior contour coordinate points, local coordinate system, fragments area and so on.

Assessment of Contour Similarity. According to the characteristics of the remains of the Dunhuang Buddhist scriptures, Zhang Yongquan [2] summarized the key factors affecting the manual conjugation work into 12 items, such as content connection and contour connection, which provided a reference for feature selection in computer-aided conjugation. Contour matching has the highest reliability and is the basis of manual conjugation, so contour similarity evaluation is very important.

Due to erosion and neglect of protection, the ancient manuscripts were worn to varying degrees, and the reliability of their features was reduced. Previous research focused on improving the matching accuracy, while the missing matching and false matching caused by strong noise are ignored. Previous researchers have shown that the Hausdorff distance can be used to solve the ancient manuscript conjugation problem, and this paper proposes an improvement based on the Hausdorff distance, which can effectively reduce the occurrence of missing matches and false matches, it is the premise of subsequent multi-feature evaluation.

Multi-layer Feature Evaluation

Physical Feature Similarity Measure. Color is a physical property of matter, but the color of ancient manuscript fragments images is not uniform because of stains and other reasons, and even the edge and the internal is not the same (see Fig. 5). Therefore, this paper chooses the color information near the conjugation position as the physical feature. In this paper, we extract the gray value near the edge of fragments, and use the gray similarity measure based on the Jacquard correlation coefficient to judge the matching condition.

The algorithm steps are as follows:

Input: Grayscale image of two fragments.



Fig. 5. Example of uneven color fragments

Step 1: After morphological denoising, Laplace operator is used to extract the contours of the current two fragments and get the points $(X1_i, Y1_i)$ and $(X2_i, Y2_i)$ on the edge of the fragments.

Step 2. Point $(X1_i, Y1_i)$ and point $(X2_i, Y2_i)$ are used to retrieve the gray value vectors of the corresponding positions of the images, which are A and B respectively.

Step 3. The Jacquard correlation coefficient $J(A, B)$ is calculated as

$$J(A, B) = \frac{|A \cap B|}{|A \cup B|} \quad (4)$$

In the formula, both $|A \cap B|$ and $|A \cup B|$ get the exact value of the set. The value of the Jacquard correlation coefficient can measure the similarity of two fragments in the physical layer. The greater the value, the higher the similarity.

Step 4. Match judgment

$$BP_y = \begin{cases} True, & \text{if } J(A, B) > PyT \\ False, & \text{elsewise} \end{cases} \quad (5)$$

In the formula, BP_y is the boolean value of the physical layer matching result, and PyT is the evaluation threshold.

Output: whether the two fragments match in the physical layer.

Semantic Feature Similarity Measure. The spacing between columns in a manuscript is called column spacing in this article. The column spacing of ancient manuscripts is remarkable and relatively stable in the same ancient manuscript. The column spacing of ancient fragments images is extracted by projection method.

The binary image (Fig. 6) is projected vertically, as shown in Fig. 6. The region with 0 value corresponds to the interval of each column, and the average value is Col.

The matching formula is as follows:

$$BSe = \begin{cases} True, & \text{if } Col > SeT \\ False, & \text{elsewise} \end{cases} \quad (6)$$

The BSe is the boolean value of the semantic matching result, and the SeT is the evaluation threshold.

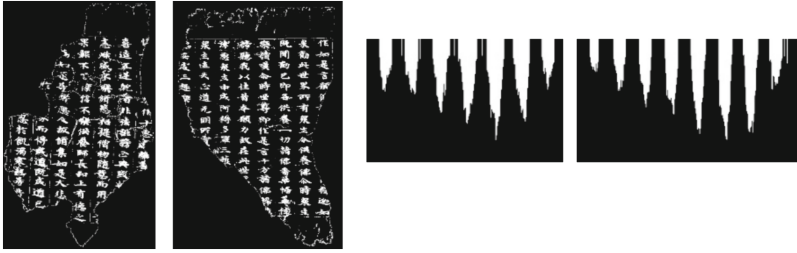


Fig. 6. Binarized ancient manuscript image and vertical projection result

3.2 Contour Similarity Measure Based on Improved Hausdorff Distance

Hausdorff distance is a measure of similarity between two sets proposed by German mathematician Feli and Hausdorff. It is widely used in image matching, pattern recognition and other engineering fields. [17] The most important feature of the Hausdorff distance is that it does not need to establish a one-to-one correspondence between the points in the set of points. Instead, the similarity between the two points is calculated by calculating the maximum distance between the two sets of points.

Given two finite sets $A = \{a_1, a_2, \dots, a_p\}$ and $B = \{b_1, b_2, \dots, a_q\}$, the Hausdorff distance between A and B is defined as follows:

$$H(A, B) = \max(h(A, B), h(B, A)) \tag{7}$$

$$h(A, B) = \max_{a \in A} \min_{b \in B} \|a - b\| \tag{8}$$

$$h(B, A) = \max_{b \in B} \min_{a \in A} \|b - a\| \tag{9}$$

$\|\cdot\|$ is a distance norm, such as the Euclidean distance used in this paper; the function $H(A, B)$ is called the directed Hausdorff distance from point set A to point set B, we define the distance from A point to a finite set as the minimum of the distance from the point to all the points in the set. Then $H(A, B)$ is the maximum of the distance from each point in point set A to point set B. Obviously, in general, $H(A, B)$ is not equal to $H(B, A)$. If $H(A, B) = D$, then the shortest distance from point A to point B in point set a is in the range from 0 to D. The Hausdorff distance $H(A, B)$ takes the maximum values of $H(A, B)$ and $H(B, A)$. By calculating the maximum values of $H(A, B)$ and $H(B, A)$, the matching degree between two point sets A and B can be obtained.

In our ancient manuscript fragment edge matching, this feature is also very good at avoiding the interference of dense corner points in the fragment edge.

Due to long-term erosion and other problems, the ancient manuscript image on the edge of the corner may not be the original tear caused, which leads to too many corner. After contour matching, some corner points can not be found on the corresponding edge, which will affect the accuracy of the matching.

The basic form of the Hausdorff distance is susceptible to sudden noise interference, that is, severe local wear at the edge of the fragments. Therefore, if we use the basic form of Hausdorff distance, the calculated results will be greatly biased, and then affect the

overall matching recognition results. We combine the ideas of Wu [16] and Zhang [17] to improve the Hausdorff distance algorithm, so that the algorithm has a certain anti-jamming ability, improve the reliability of the algorithm, the improvement is divided into three aspects:

- a) Firstly, the calculated values D_i are arranged in order from large to small, resulting in a new data set $\{D_i \mid 1 \leq i \leq N\}$, where D_1 is the most, large, and D_N is the least. Secondly, calculate whether the parameter K_i exceeds the threshold K_{set} :

$$K_i = \frac{D_i^* = D_{i+1}^*}{D_{i+1}^* - D_{i+2}^*} > K_{set} \quad (10)$$

- b) Considering that the Hausdorff distance of a single point is easily affected by noise, we use the modified Hausdorff distance (MHD). In Zhang's research [17], it is also proved that MHD is not sensitive to noise and can avoid the deviation caused by partial noise. The definition is as follows:

$$h(A, B) = \frac{1}{N_A} \sum_{a \in A} \min_{b \in B} \|a - b\| \quad (11)$$

- c) In addition to the improvement of the Hausdorff distance, we also introduce the feature of tilt angle. After obtaining the set of coordinates V of the outer contour of fragments I , the unit vector along the x direction of the coordinate axis is x_0 , the vector for the inclination of the line segment between V_{k-1} and V_k is expressed as δ_k in the local coordinate system:

$$\cos \delta_k = \frac{P_k \cdot x_0}{\|P_k\| \times \|x_0\|} \quad (12)$$

2.3.1 experiments show that the tilt angle feature can effectively reduce the occurrence of false matching.

The improved method is suitable for the conjugation scene of ancient manuscript fragments, and can effectively avoid the misjudgment problem caused by edge information distortion.

4 Experiments and Results

4.1 Experimental Environment

The experiments were programmed in Pycharm2021 and Python3.6 and completed on the IW4210-4G model GPU server.

4.2 Data Set of Dunhuang Ancient Manuscript Fragments

In order to quantitatively evaluate and analyze the model in this article, the Dunhuang ancient manuscript fragments dataset is divided into two parts. One is the rejoinable fragment group sorted according to the existing professional literature related to Dunhuang research. It has 11 groups, with a total of 31 pieces. The other part is 225 solitary pieces without matching items. These fragments are used as experimental interference items, with a total of 256 pieces.

4.3 Experimental Results

Contour Similarity Evaluation. As shown in Fig. 7, fragments S9040 and S9069 are the correct match combination, but the matching segment shown by the contour similarity measure match result (the line segment in the box in the figure) is incorrect.

Because of the abundant contour information of ancient fragments, only considering the contour similarity may lead to the false matching caused by the contour information approximation. To reduce the occurrence of such false matching, this paper incorporates the feature of tilt angle sequence into the measurement of contour similarity. The experimental results, as shown in Fig. 7, demonstrate that fragments s9040 and s9069 were able to successfully identify the correct matching segment (indicated by the line segment within the boxed area in the figures) after the inclusion of the tilt angle sequence feature.

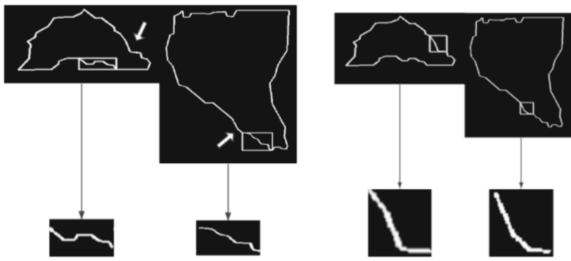


Fig. 7. Matching results without the introduction of the tilt angle feature (left) and Matching results by adding the Oblique sequence features (right)

In order to verify the effectiveness of the improved Hausdorff distance-based contour similarity evaluation for contour similarity assessment, we compared it with other algorithms for contour similarity evaluation using the improved Hausdorff distance [13–15].

Algorithm 1 is an automatic irregular cultural relic fragment conjugation algorithm based on corner features [13]. The paper proposes a new conjugation process that firstly performs coarse matching based on angle values, followed by fine matching based on edge length values. It uses an improved local matching method suitable for polygon features to find spatially adjacent fragment pairs and measure the degree of matching. By generating a global path and conjugating the fragments according to the path, the conjugation of multiple fragments is achieved. Algorithm 2 segments the target contour and uses partial Hausdorff distance to measure the distance of each segment [14]. By scientifically synthesizing the partial Hausdorff distances of each segment, a distance measure for the target contour is designed, and the target type is determined based on the principle of minimum distance. Algorithm 3 achieves fast matching and conjugation of fragments by applying rigid transformation to the contour information [15]. Additionally, the algorithm measures the consistency of contour coordinates and the shape of the outer circular contour to evaluate the matching error and conjugation effect. Algorithm 4 is our improved contour similarity evaluation algorithm without incorporating the tilt angle feature, while Algorithm 5 is our improved contour similarity evaluation algorithm that includes the tilt angle feature. The experimental results are shown in Fig. 5. For contour

similarity measurement, this paper adopts the top k accuracy to evaluate the performance of algorithm searching for reliable matching candidates, representing the inclusion of correct matching items among the top k ranked matching items.

Table 1. Comparison of different algorithm

Algorithm	Top 1 Accuracy	Top 3 Accuracy	Top 5 Accuracy
Algorithm 1 [13]	41.90%	61.29%	67.74%
Algorithm 2 [14]	58.06%	70.97%	80.65%
Algorithm 3 [15]	45.16%	64.52%	70.97%
Algorithm 4	70.97%	83.87%	87.10%
Algorithm 5	77.41%	90.32%	100%

According to Table 1, Algorithm 4 has improved the top 1 accuracy by 29.07%, 12.06%, and 25.81% compared to the other three algorithms, respectively. It has also improved the top 3 accuracy by 22.58%, 12.90%, and 19.35% compared to the other three algorithms, respectively. In terms of top 5 accuracy, Algorithm 4 has improved the other three algorithms by 19.36%, 6.45%, and 16.73%, respectively. The improvement in the top 1 accuracy metric demonstrates that Algorithm 4 can effectively avoid false matches compared to the other three algorithms. The improvement in the top 3 and top 5 accuracy metrics demonstrates that Algorithm 4 can effectively avoid missing matches compared to the other three algorithms.

Algorithm 5 has improved by 6.44% in top 1 accuracy compared to Algorithm 4. It has also shown an improvement of 6.45% in top 3 accuracy and 12.9% in top 5 accuracy compared to Algorithm 4, thus demonstrating the effectiveness of introducing tilt angle features.

Multi-layer Feature Evaluation. It is also possible that the high similarity of contour information between fragments is a false match, so further evaluation is needed after the contour similarity measurement is completed. The improved Hausdoff distance is used to represent the degree of matching of each matching segment, arranged in order of its value from small to large. The smaller the value, the more matching the contour information of the two fragments. Table 2 shows the contour matching results of fragment S8983.

According to Table 2, the most suitable fragment for S8983 is S9081, judged by its contour features. But the real matching fragment should be the second-ranked S8961, so we know that the matching fragment based only on the contour features is the wrong match result. As you can also see from Fig. 8, there are similarities in the edge contours (in the box) between S8983 and S9081, but the correct match is S8961.

It is obvious that only contour feature matching can not eliminate false matching effectively, so this paper adds multi-layer feature fusion for further matching and evaluation, and improves the accuracy by adding feature filtering. Taking column spacing

Table 2. Result table of contour similarity measurement for s8983.

Rank	Fragment number	Hausdoff distance
1	S9081	9.7778
2	S8961	13.0909
3	BD9428	15.3846
4	Or15012	17.6741
5	Or9912	23.8092

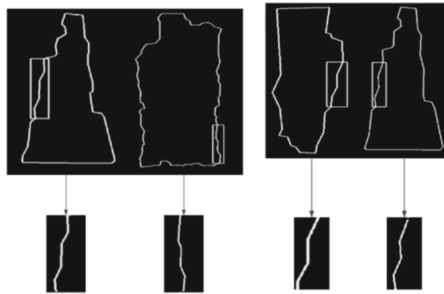


Fig. 8. False matching (left) result of Fragment S8983 (left) and S9081 (right) and true matching (right) result of Fragment S8961 (left) and S8983 (right)

consistency as an example, Table 3 shows the results of column spacing extraction for the five fragments in Table 2.

Table 3. Results of Column space

Fragment number	Column spacing	Column spacing difference between S8983 fragment and other fragments
S8961	16	1
S9081	30	15
BD9428	26	11
Or15012	27	12
Or9912	17	2

The results show that the S8983 fragment and the S9081 fragment have a large column spacing difference, which does not meet the matching requirements, while OR9912, which also has a small column spacing difference, does not perform well in the contour matching phase. Therefore, the only matching fragment is S8961 by combining the contour matching results and the column spacing consistency results, which is in line with the actual situation and shows the necessity of multi-layer feature fusion.

Analysis of Experimental Results. In this paper, Partial Accuracy and Complete Accuracy are used as the evaluation indexes of the whole model. Partial Accuracy is the rate of incomplete matching (including the case that the elements in the group are not found completely), complete Accuracy is the rate of Complete matching (all fragments in the group are found and no fragments is mixed into the success).

Based on the experimental results, when calculating Complete Accuracy in terms of groups, we can find 9 groups and 221(Group) isolated fragments. In total, we can output 236 groups, and the Complete Accuracy is 97.45%. The Partial Accuracy was calculated in units of pieces. There were 9 groups (25 pieces) that could be found completely, and 2 groups (4 pieces) that could not be found completely. The number of isolated fragments found was still 221, and the total number of fragments was 256. Then the Partial Accuracy was calculated to be 97.67%.

Ablation Experiments. To verify the effectiveness of various hierarchical features and their degree of influence on the final suffix conjugation results, we conducted comparative experiments on individual hierarchical features, pairwise combined hierarchical features, and three hierarchical feature combinations. The results are shown in Table 4, where *py*, *st*, and *se* respectively represent the physical layer, structural layer, and semantic layer.

Table 4. Comparison of reconstruction properties of different layer combinations

Layer combinations	Complete Accuracy	Partial Accuracy
<i>Py + St + Se</i>	97.45%	97.67%
<i>Py + St</i>	96.19%	94.92%
<i>St + Se</i>	93.22%	94.53%
<i>Py + Se</i>	92.14%	87.89%
<i>Py</i>	92.14%	87.89%
<i>St</i>	92.37%	93.75%
<i>Se</i>	57.48%	29.30%

Note: The black font indicates the optimal result

From Table 4, it can be seen that the effectiveness of the physical layer and structural layer is significantly higher than that of the semantic layer feature. The reason for this may be that ancient writing had clear regulations on character spacing, and simple inter-column spacing features were not highly distinctive. From the perspective of the fusion of two-layer features, the success rate of conjugation has been improved. In terms of the fusion of two-layer features, the success rate of conjugation has been improved. Although the semantic layer features have become subordinate to other layers, it has not led to an increase in missing matches. From the experimental results of the fusion of three-layer features, the inclusion of the semantic layer has achieved the optimal outcome, indicating that the use of semantic layer features is effective in reducing false matching. The experimental results indicate that each layer of features in the model has a positive

impact on the success of conjugation. When all features are fused, the consistency and complementarity of multiple layers of features are fully utilized, resulting in the best conjugation effect. This demonstrates the necessity of multi-feature fusion and the rationality of algorithm design.

5 Conclusion

Currently, the most advanced computer technology has not yet been utilized in the practice of conjugating ancient manuscript fragments. Due to the high degree of heterogeneity and irregular edges of these fragments, matching based solely on contour features results in low accuracy. This paper proposes an improved Hausdorff distance-based contour similarity evaluation index and evaluation method. Additionally, due to the damage, corrosion, fragmentation, staining, and even partial loss of ancient manuscript fragments, the matching task is complex and accuracy is low when relying on a single feature. To address this, a fully automatic multi-feature fusion conjugation model is proposed, which includes contour, physical, and semantic layer features. This model improves the success rate of patching and allows the entire conjugation process to be completed automatically without intervention.

This article presents an analysis of the contour similarity algorithm using Dunhuang manuscript fragments as an example. The results demonstrate that the improved contour similarity evaluation indicators and methods are feasible and can effectively reduce the amount of false matching. Additionally, the article completes the algorithm implementation and model evaluation of a multi-feature fusion fully automatic conjugation model. Compared with other algorithms, the fusion model can extract multi-level features, thereby improving the description level of the fragments, reducing missed and incorrect judgments during the conjugation process, and improving the accuracy of the conjugation. The accuracy of the fusion model on the Dunhuang manuscript fragment dataset can reach 97.45%, effectively improving the success rate of conjugation.

References

1. Leitão, H., Stolfi, J.: A multiscale method for the reassembly of two-dimensional fragmented objects. *IEEE Trans. Pattern Anal. Mach. Intell.* **24**, 1239–1251 (2002)
2. Zhang, Y.Q., Luo, M.J., Zhu, R.X.: Exploring the dunhuang sutra cave riddle. *Soc. Sci. China* (03), 180–203+208 (2021)
3. De Smet, P., De Bock, J., Corluy, E.: Computer vision techniques for semi-automatic reconstruction of ripped-up documents. *Visual Inf. Process.* **6**, 189–197 (2003)
4. Kong, W.X., Kimia, B.B.: On solving 2D and 3D puzzles using curve matching. In: *Proceedings of the 2001 IEEE Computer Society Conference on Computer Vision and Pattern Recognition, CVPR 2001*, vol. 2, p. 2 (2001)
5. Liu, Q.J., Chen, P.: Algorithm design on scraps of paper splicing based on text feature. *Res. Explor. Lab.* **35**, 11 (2016)
6. Liu, X.G., Jia, Z.Y., Liu, W.J., Han, M.: Study of document recovery method based on gray-level matrix. *Appl. Res. Comput.* **33**(12), 3901–3904+3908 (2016)
7. McBride, J.C., Kimia, B.B.: Archaeological fragment reconstruction using curve-matching. In: *2003 Conference on Computer Vision and Pattern Recognition Workshop*, vol. 1, p. 3 (2003)

8. Papaodysseus, C., Panagopoulos, T., Exarhos, M., Triantafillou, C., Fragoulis, D., Doulas, C.: Contour-shape based reconstruction of fragmented, 1600 BC wall paintings. *IEEE Trans. Signal Process.* **50**(6), 1277–1288 (2002)
9. Tsamoura, E., Pitas, I.: Automatic color based reassembly of fragmented images and paintings. *IEEE Trans. Image Process.* **19**(3), 680–690 (2010)
10. Lu, Y.H.: A method of fragment splicing restoration under minimal human intervention. *China Comput. Commun.* **14**, 51–54 (2017)
11. Luo, Z.Z.: Semi-auto stitching of scrapped paper based on character characteristic. *Comput. Eng. Appl.* **48**(05), 207–210 (2012)
12. Zhang, K., Li, X.: A graph-based optimization algorithm for fragmented image reassembly. *Graph. Models* **76**(5), 484–495 (2014)
13. Shi, B.Z.: An algorithm for automatic stitching of irregular cultural relics based on corner features .Master's thesis. Inner Mongolia Agricultural University (2019)
14. Wang, X., Jiang, S.B., Zhang, X.M.: SAR target contour matching and its application in target recognition. *Comput. Eng. Design* **40**(01) (2019)
15. Shang, C., Cao, L.G.: Research on two-dimensional mosaic algorithm of ceramic fragments based on shape metrics. *J. Ceramics* **42**(02) (2021)
16. Wu, Y.M., Fan, Y.P.: Multi-terminal hybrid direct current transmission line protection scheme based on traveling wave theory and improved Hausdorff distance. *J. Wuhan Univ. Sci. (Eng. Edition)*
17. Zhang, L.G., Wu, J.Q.: Gesture recognition based on Hausdorff distance. *Chin. J. Image Graph. A* **7**(11), 1144–1150 (2002)